Slow weathering in a sandstone-derived Podzol (Falkland Islands) resulting in high content of a non-crystalline silicate

Javier Cuadros[1], Mara Cesarano[1,2], William Dubbin[1], Stuart W. Smith[3,*], Alexandra Davey[3,#], Baruch Spiro[1], Rodney G.O. Burton[4], Anne D. Jungblut[5]

[1] Department of Earth Sciences, Natural History Museum, London W7 5BD, UK

[2] Dipartimento di Scienze della Terra, dell'Ambiente e delle Risorse, Università degli Studi di Napoli ''Federico II'', Italy

[3] Falklands Conservation, Jubilee Villas, Ross Road, Stanley, FIQQ 1ZZ, Falkland Islands

[4] Environmental Consultant, Cambridge, UK

[5] Department of Life Sciences, Natural History Museum, London W7 5BD, UK

Short title: Slow weathering produces soil with high non-crystalline content

Corresponding author: Javier Cuadros; j.cuadros@nhm.ac.uk

[*] Presently at the Department of Biology, Norwegian University of Science and Technology, 7491 Trondheim, Norway.

[#] Presently at Conservation Science Department, Royal Botanic Gardens, Kew, Millennium Seed Bank, Wakehurst Place, Ardingly, West Sussex, RH17 6TN, UK.

Abstract

Mineral weathering processes in soils are important controls on soil characteristics and on bio- and geochemical cycling. Elucidation of these processes and their mechanisms is crucial for understanding soil environments and their influence globally. An Umbric Podzol from the Falkland Islands was studied while investigating possible ways to counteract soil degradation and loss. The soil had lost the O, E and Bs horizons through erosion, thus revealing the transitional B/C horizon, which grades into the underlying parent material. Samples were taken from the B/C surface and 5 cm below the surface, then analyzed with X-ray diffraction, scanning electron microscopy with energy-dispersive X-ray spectroscopy, organic C and N analysis, and analysis of extractable Fe and Al with the dithionite-citrate-bicarbonate and ammonium oxalate methods. The soil fabric and mineralogy were compatible with derivation from sandstone rock. Clasts of heterogeneous mineral composition as well as loose material from disaggregated clasts were present. The soil had large proportions of quartz and albite, and minor amounts of muscovite, chlorite, plagioclase, feldspar, kaolinite, all showing signs of chemical alteration, and non-diffracting Fe oxide (goethite and/or ferrihydrite). The most peculiar characteristic was a large component of a silicate gel of small particle size (< 1 μm), non-extractable, with heterogeneous composition. The average composition of this gel is similar to that of the bulk soil and approaches that of Al-Fe-rich smectite. The silicate gel is formed partly by the translocation of metals from O, E and Bs horizons and partly by dissolution of the primary minerals of the B/C horizon, both of which precipitated in combination with low water mobility causing fast saturation of the interstitial water. There are no reports of silicate gels with these characteristics or abundances from soils or other weathering environments. Thus, our observations indicate the existence of complex, successive weathering steps not yet identified that could be investigated in materials subjected to slow weathering such as the soil described here.

Keywords: Falkland Islands, non-crystalline silicates, Podzols, weathering.

INTRODUCTION

Silicate weathering

Weathering of silicate rocks in soils and other environments is a much studied process, with significance for global geochemical and bio-geochemical cycles. The accurate knowledge of the nature of weathering products is important to know (1) how weathering takes place, (2) the chemical balance during weathering, (3) the kinetics of the weathering process and relative stability of successive weathering phases, and (4) the interaction of minerals with the biosphere and bioavailability of nutrient elements. Weathering depends on a great range of variables including the rock type, porosity, water composition, water regime, pH, temperature, slope, biological activity and the modifications of physical conditions generated by the micro- and macro-biota, many of which variables are intimately linked to one another (Anderson et al., 2007; Chorover et al., 2007). All these and other factors generate a wide range of weathering intensity and products, from the absence of weathering to the substitution of the initial minerals by those at the very end of the weathering sequence, dominated by Al and Fe oxides and quartz (Chamley, 1989).

Within the series of weathering products, silicate phases are typically crystalline. New minerals are generated from the previous ones through several routes and mechanisms. Poorly crystalline silicate phases are an ephemeral stage of the weathering process (Wilson, 2004). They are found in young volcanic soils, mainly as allophane, imogolite and their precursors, where the abundant original tephra has evolved only to a stage of partial element redistribution and crystal order (Wada, 1989). Non-crystalline silicate phases are found very frequently as intermediates between the original phases and the newly-formed ones, but almost universally in very small amounts only detectable with microscopic techniques and placed between parent and product phases, all of which attest to their short-lived existence (Wilson, 2004). Generally, microbial action precipitates secondary silicate phases of lower crystal order than abiotic environmental conditions. This is perhaps because crystallization takes place within biofilms and on biological substrata, environments that can reach

higher solute supersaturation (that leads to fast precipitation) given their viscosity, or because the environmental conditions have steeper physical and chemical gradients (heterogeneous environments favoring formation of small particles) (e.g., Konhauser et al., 1993). However, to our knowledge, there are no reports of major formation of non-crystalline silicate phases, i.e., that can be detected macroscopically, produced by microbially mediated weathering. There exist reports of relatively abundant poorly crystalline silicate phases in soils, which can be dissolved and measured by standard extraction methods. There is no obvious connection between the occurrence of such phases and the specific characteristics of the soils (e.g., Mitchell and Farmer, 1962; McKeague and Brydon, 1970). This fact is not surprising considering the numerous factors that affect weathering reactions and their many possible combinations that can obscure links between causes and effects.

Podzols are zonal soils mainly of temperate and boreal regions found under coniferous forest or ericaceous vegetation. They usually form from coarse textured and unconsolidated siliceous materials such as quartz-rich sands and sandstones or from the sedimentary debris originating from granitoid rocks. Podzolization is the pedogenic process involving the weathering and subsequent translocation of Al, Fe and organic matter to form a spodic horizon (Buurman and Jongmans, 2005; Sauer et al., 2007). The two main processes involved in podzolisation are (i) cheluviation, the downward movement of Al- and Fe-organic chelates and (ii) chilluviation, the subsequent accumulation of the metal chelates as precipitates to form the illuvial spodic horizon. The Al and Fe thus deposited in this illuvial horizon typically precipitate as short-range ordered silicate phases (e.g., allophane, imogolite) (Wada, 1989), Fe(III) oxides (e.g., ferrihydrite) (McKeague et al. 1983), or as crystalline secondary phases such as smectitic clays (Egli et al., 2002). Silica gels possessing no defined structure have also been observed in Podzols in minor amounts, decreasing with depth (Saccone et al., 2008).

Here we report for the first time the unusual finding of an eroded Podzol (horizons above B/C are missing), derived from sandstone in the Falkland Islands, consisting of the original minerals, slightly weathered, and a large amount of a silicate gel with the following characteristics: (1) The gel is not affected by usual methods of extraction of non-crystalline phases, (2) it does not diffract X-rays, (3) it has local heterogeneous composition and an average chemistry approaching that of an Al-Fe smectite. These characteristics and large preservation of the sandstone fabric in the exposed B/C horizon indicate, in particular, the arrest of the processes leading to formation of crystalline alteration products and, more generally, a slow weathering process in this horizon. If this type of slow weathering is found to be relatively abundant it might show complex weathering processes usually missed due to their fast rate.

Geologic setting

The Falkland Islands form an archipelago located in the South Atlantic Ocean, between 51°S and 53°S and 57°30′ W and 61°30′ W, approximately 650 km east from the Strait of Magellan, South America. The islands consist of two mainlands, West Falkland and East Falkland, and over 700 smaller islands (Aldiss and Edwards, 1999). The terrains with outcrops in the islands are divided in four main groups according to their age:

(1) Mesoproterozoic (1120-1000 Ma) granite and gneisses of the Cape Meredith Complex. These rocks only crop out in a coastal section of Cape Meredith, the southern extreme of West Falkland (Aldiss and Edwards, 1999).

(2) Silurian to Devonian sedimentary rocks of the West Falkland Group. This group underlies most of West Falkland and the adjacent islands, as well as the northern part of East Falkland and Beauchêne Island (Aldiss and Edwards, 1999). It consists mainly of sandstones, with subordinate quartzite, siltstones and mudstones. This group has been divided into four formations which

represent different depositional environments (i.e., fluvial to deltaic and marine shelf). From the oldest to the youngest they are: Port Stephens Formation, Fox Bay Formation, Port Philomel Formation, and Port Stanley Formation (Aldiss and Edwards, 1999).

(3) Carboniferous to Permian sedimentary rocks of the Lafonia Group. This group is widespread in Lafonia, southern East Falkland, and the rest of this island. It also occurs in West Falkland, on the east flank of the Coast Ridge (east coast of the island) as well as in Port Purvis (NE) and the east end of Byron Sound (NW) (Aldiss and Edwards, 1999). This group consists of sequences of sedimentary strata including fine grained sandstones, siltstones, mudstones, rare tuff and thick tillite (Aldiss and Edwards, 1999). Five formations belong to the Lafonia Group, from older to younger: Bluff Cove Formation, Fitzroy Tillite Formation, Port Sussex Formation, Brenton Loch Formation, and Bay of Harbours Formation. They are the product of major glaciations, followed by basinal, turbiditic and deltaic sediments.

(4) Jurassic igneous intrusions cropping out mainly in West Falkland and some adjacent islands (Aldiss and Edwards, 1999). Some intrusions also occur in East Falkland. These rocks, mainly dolerite dykes, have been subdivided into seven groups according to their orientation, distribution and field character.

The studied soil is from an area near Fitzroy Farm, central East Falkland (Figure 1). The underlying rocks are sedimentary of the Fitzroy Tillite Formation (Carboniferous to Permian), deposited in Gondwana during a glacial episode (Stone, 2011). The Fitzroy Tillite Formation consists of massive sandy diamictite, with intercalated mudstones and small sandstone bodies. It crops out in East Falkland where it overlies the Bluff Cove Formation, and along the east coast of West Falkland (Aldiss and Edwards, 1999). It comprises a wide range of lithologies dominated by quartzite and sandstone, less abundant but important various granites, and accessory components represented by a

wide range of igneous and metamorphic rocks and sandstone (Stone, 2011). In spite of the absence of striated rock surfaces, the Fitzroy tillites have been interpreted as sub-glacial deposits in West Falkland, whereas they are considered marine tillites in East Falkland (Stone et al., 2012).

The extent of recent glacial processes across the islands is debated. Cruickshank (2001) reported that the islands were not covered by ice in the last glaciation (14-25 Ka BP). This view corroborates that of Aldiss and Edwards (1999), who considered that the soft sediment deformation observed in parts of the islands represents the result of slumping on depositional slopes, rather than ice movement or melting. There is positive evidence of Pleistocene glacial features, such as small cirques and ice-eroded valleys, in the mountains (Clapperton, 1971; Clark, 1972; Wilson et al., 2008). However, these features appear to be much older (46-827 Ka) than the last glaciation (Hodgson et al., 2014). Authors agree about the evidence of periglacial processes that resulted in landscape features such as dropstones (Adie, 1952; Clark, 1976; Wilson et al., 2008), stone runs (Hansom et al., 2008), and rock-weathering (Wilson, 1994). The ages of stone runs measured by Wilson et al. (2008) were older than the last glaciation (42-800 Ka), whereas Hansom et al. (2008) measured stone run ages from in excess of 54 Ka to 16 Ka or younguer, thus including the last glaciation. Clark et al., (1998) found sediments from solifluction and landslides produced in a periglacial environment covering organic-rich sediments 28-36 Ka old. Further relevant evidence is provided by Clark and Wilson (1992), who described ventifacts generated immediately before 11-13.6 Ka BP, following a period of intense cold. For Clark (1976), the periglacial Falklands landscape was sculpted in a dry climate. From all the above evidence it can be safely concluded that glacial activity in the Falklands during the Pleistocene decreased in intensity from ~800 Ka BP. Old glacial features have been preserved through several glacial periods and the features generated in the last glaciation are mainly periglacial.

Climate

As indicated above, it is possible that mountains in the Falklands had a permanent ice cap during the last glaciation, indicating a climate significantly colder than the present one. Now, climate in the Falklands is cold/temperate/oceanic. Technically, it corresponds to ET (Tundra climate) in the Köppen-Geiger classification, with the extreme NW area of the islands defined as Cfc (Subpolar oceanic climate) (Climate-Data.org, 2016). The months with the highest and lowest temperatures are January and July, with the corresponding average values of 9.4 and 2.2 °C, respectively. Ground frost can occur throughout the year. The rainfall is irregularly distributed across the islands and strongly seasonal, with a mean annual precipitation of 640 mm recorded at Stanley, East Falkland and ~36 km northeast of the investigated area (climate data recorded 1961-1990; McAdam, 2013, 2014). In the study area (Figure 1) the rainfall distribution is as follows. Spring and autumn have average precipitation < 150 mm, while summer and winter have 150-200 mm (Jones et al., 2013). As an oceanic island the Falklands experiences strong winds with average wind speeds of 8.5 m s^{-1} (16.5 knots) and frequent gale-force winds (Jones et al., 2013). It has been considered that the strong winds and centuries of extensive sheep grazing and burning, has produced a mainland vegetation dominated by low stature swards of the grass *Cortaderia pilosa* (whitegrass) and the dwarf shrubs *Empetrum ruburum* (diddle-dee), *Baccharis magellanica* (christmas bush) and *Chiliotrichum diffusum* (fachine) (McAdam, 2014). However, analysis of pollen dating 28-36 Ka BP, before the last glaciation, indicates a vegetation similar to the present one, dominated by grasses (Clark et al., 1998). Thus, human activity may have had little or no effect on the Falklands vegetation.

Soils

Soils of the Falkland Islands are dominated by Podzols with sapric or fibric surface horizons containing more than 20% organic carbon (Cruickshank, 2001). Following Cruickshank (2001), a typical Falklands podzolic profile comprises, from top to bottom, a peaty O horizon (generally up to 30-38 cm), a thin leached E horizon (5-10 cm), and an incipient or consolidated iron pan (1-2 cm

thick) overlying a poorly drained silty clay podzolic B horizon. The peaty O horizon and the iron pan are often laterally discontinuous. The pH of the profile is acidic and increases from average values of about 4.5 in the O horizon to 5.2 in the podzolic B. The podzolic Bs horizon contains 35-60 wt% of clay-sized material (Cruickshank, 2001). The irregularly distributed precipitation during the year causes soils to be moisture-deficient in the spring and also, but less so, in the summer (Upson et al., 2016).

The investigated soil is an eroded Umbric Podzol (IUSS Working Group WRB, 2015) and lacks above-ground vegetation due to the combined effects of sheep overgrazing and erosion (Wilson et al., 1993). Intense erosion has also removed the O, E and Bs horizons thus exposing the B/C horizon (as described by Cruickshank, 2001; Appendix Figure A.1 shows the complete soil profile, adjacent to the studied area). Our sampled soil lacked the iron pan frequently found elsewhere in the islands and there was no apparent gleying in the Bs horizon (Appendix Figure A.1). The soil is rich in fine-grained material, light yellowish brown (10YR 6/4), and contains numerous cm-size fragments of sandstone heavily eroded by wind, which gives many of these fragments a flat shape (Appendix Figure A.2). Average soil pH from the surface to a 5 cm depth was 5.2 (see below).

METHODS

The soils were sampled in November 2013 at the location 51° 48’ 47.69’’ S 58° 20’ 52.63’’ W (Figure 1), over an area of ~16 m × 16 m, up to a depth of 5 cm. The soil pH was measured placing samples in the minimum necessary amount of distilled water and using a Mettler Toledo MP 225 pH meter. A total of 48 measurements were made distributed across the investigated area and up to 5 cm. The resulting pH values ranged 4.6-5.9 and averaged 5.2. Thirty two samples (~200 g each) were obtained at similar intervals covering the mentioned area, 16 from the surface (0-2 cm) and 16 from 5 cm (5-7 cm) below the surface (not below the surface samples but in different spots). Sample aliquots were finely ground with an agate pestle and mortar.

The organic C and N of all the soil samples were analyzed using a “vario EL cube” model from Elementar. Ground samples of ~10 mg each were placed in Ag foil capsules, treated three times with increasingly concentrated HCl (2, 4 and 8% v/v) to remove carbonates and then dried. They were then wrapped in the Ag capsule, introduced in the C-N analyzer and flash-heated at 1150 °C. Samples were analyzed in duplicate or triplicate as required (due to variability of the results). Two reference materials, Sandy Soil Standard (Elemental Microanalysis Ltd) and High Organic Sediment Standard (Elemental Microanalysis Ltd), were analyzed with the samples and gave results within the certified values.

The ground soil samples were analyzed with X-ray diffraction (XRD). First, all of them were analyzed as random powders. The samples were side-loaded in holders and analyzed between 2 and 80 °2θ in a PANalytical X’Pert diffractometer with Cu radiation. This apparatus is equipped with an X’Celerator solid-state linear detector that continuously integrates intensity in an angle of 2.1°2θ. The powders were analyzed for 1 h, with an effective step size of 0.0167 °2θ and corresponding counting time of 99.7 s per step. Other conditions were: 45 kV and 40 mA current, 0.02 rad Soller slit, 0.5° antiscatter slit, 0.25° divergence slit, and Ge monochromator.

Because the soils were mineralogically homogeneous, only 3 samples were investigated as oriented mounts. The fraction < 2 μm was separated by dispersing the soils in deionized water, sonicating the dispersions for ~3 min in a bath, letting the suspension to sediment and collecting the upper part of the dispersion (top 2 cm after 128 min sedimentation). The dispersion with the fraction < 2 μm was placed on a glass slide and let dry. The air-dry oriented mounts were investigated with the same diffractometer and conditions, except that analyses were in the ranges 2-40 and 2-15 °2θ, with an effective counting time of 200 s per step (1 h analysis for 2-40 °2θ, 20 min analysis for 2-15 °2θ).

The oriented mounts were then glycolated at 60 °C in an ethylene glycol atmosphere overnight and analyzed as indicated above.

Extractable Al and Fe were measured in four samples only because they appeared to be homogeneous morphologically and mineralogically. The dithionite-citrate-bicarbonate (DCB) and ammonium oxalate (AO) methods were used, following Shang and Zelazny (2008). The DCB method is expected to extract Fe from all Fe(III) oxides and oxyhydroxides, crystalline or non-crystalline, and the Al associated with these phases. The AO method is expected to extract only Fe and Al in non-crystalline oxide and oxyhydroxide phases. For the DCB treatment, 100 mg of soil were suspended in 5 mL of 0.3 M $C_6H_5Na_3O_4 \cdot 2H_20$ (sodium citrate) and 0.5 mL of 1 M $NaHCO_3$ adjusted to pH 8.5. The reaction vessels were then placed in a water bath (80 °C) and 0.1 g of $Na_2S_2O_4$ (sodium dithionite) was introduced to each reactor. Following a 2 h reaction, with intermittent stirring, the supernatant solutions were obtained by filtration and analyzed for Fe and Al by ICP-OES (Thermo iCap 6500 Duo). For the AO method, 100 mg of each soil were reacted with 40 ml of 0.2 M $(NH_4)_2C_2O_4 \cdot H_2O$ (ammonium oxalate) in the dark at pH 3 as described by Shang and Zelazny (2008). Following a 4 h reaction the supernatant solutions were obtained by filtration and analyzed for Fe and Al by ICP-OES. All samples, for both CBD and AO extractions, were analyzed in duplicate.

A thin section was prepared with one of the pristine soil samples (whole sample, not ground) to investigate the fabric and composition with scanning electron microscopy and energy dispersive X-ray spectroscopy (SEM-EDS). A portion of the soil containing aggregates of several mm size was embedded in Epoxy resin while heating gently to decrease the resin viscosity and facilitate penetration within the soil pores. After hardening, the block was glued to a glass slide and polished up to ~30 μm thickness. Additionally, the soil fraction < 2 μm was investigated with SEM-EDS in two samples. One corresponded to the < 2 μm fraction of the soil and the other to the < 2 μm size

fraction of the soil after extraction of amorphous Fe and Al with AO. For these samples, the < 2 μm fraction was separated as indicated above and prepared as sediment on a resin block. For this, a few drops of the water dispersion containing the < 2 μm size fraction was placed on the resin block and let dry. All samples (thin section of whole soil and mounts with the fraction < 2 μm) were C-coated and analyzed in a Zeiss Ultra Plus Field Emission microscope equipped with an Oxford EDS micro-analysis detector and INCA software, using back-scattered and secondary electron detectors. The study was carried out at 10 and 20 kV. For the EDS analysis, acquisition time was 30 s, with ~12% dead time. Chemical analyses were corrected for the element k factors with mineral standards. The thin section of the whole soil was chemically analyzed in two ways. First, three areas of different morphology, comprising different proportions of cohesive grains and loose material, were selected, one of 1000 μm × 750 μm and two of 500 μm × 375 μm. For these areas the complete chemical composition map was acquired. Second, individual mineral grains were analyzed in point analysis mode. Calculations using the program CASINO (Drouin et al., 2001, 2007) indicate that the diameter of the analyzed spot was always < 200 nm, and the depth varied between 1 μm (10 keV) and 3 μm (20 keV). In the sediments from the < 2 μm fraction samples, the individual grains were typically analyzed in point ananlysis mode. There was also a very fine material which was analyzed selecting rectangular areas that ranged from a few μm to ~30 μm by side. In this way, the composition of tens to thousands of very fine mineral grains was averaged in each analysis.

RESULTS

Organic C and N concentrations

Organic C and N for the 32 samples ranged 0.3-1.5 wt% C, and 0.02-0.09 wt% N, with a positive correlation between the two (R^2 = 0.73). The average organic C content for all samples was 0.69 wt% and the C/N ratio varied from 11 to 18. In Podzols, the organic C profile shows two areas of concentration, the O horizon and the podzolic B horizon, while the E horizon is largely depleted of organic C. The B/C horizon, as it grades into the parent material, typically has an organic C content

intermediate between those of the E and podzolic B horizons. In a study of 171 Podzols from Canada, Evans and Cameron (1985) measured an average of 2.64 wt% organic C in the podzolic B, a figure that included the organic-C rich Bhs horizons and the C-poor Bs horizons. Meanwhile the eluvial E horizon of Podzols typically holds ~0.5 wt% organic C (Sauer et al., 2007). Therefore our value of 0.69 % is coherent with organic C levels in the B/C horizon, our sampling depth. The C/N-ratio of Podzols varies with depth and is typically 20 to 50 in the O horizon, decreasing to 10 to 15 in the E horizon, then increasing again to 15 to 25 in the podzolic B horizon. Our measured C/N ratio of 11 to 18 for the B/C horizon is broadly consistent with the above C/N trends.

X-ray diffraction

The results from XRD were homogeneous for all samples. They consist mainly of quartz with minor albite, K-feldspar, muscovite, chlorite and kaolinite, as indicated by the intensity of the XRD peaks of the several phases (Figure 2a). There are also non-crystalline Fe oxides as indicated by the light brown color of the soils (see below for further evidence). This mineralogy is coherent with the soil originating in the Fitzroy Tillite formation, with sandstone as the major or only component as indicated by the predominance of quartz and albite (Figure 2a). The fraction < 2 μm was abundant, in agreement with the previous report of abundant clay-sized material in many of the Falkland soils (Cruickshank, 2001). The investigation of this fraction (< 2 μm) as oriented mounts produced the surprise that the large majority of this material was not crystalline (Figure 2a). Only very minor chlorite, mica and kaolinite (Figure 2b; see below for the evidence of kaolinite presence) could be detected, which indicated that most of the thick sediment in the preparation was not diffracting X-rays. No smectite or any swelling phyllosilicate were present (Figure 2b). Apparently, then, a large component of the investigated soil was an intriguing non-crystalline inorganic phase.

Extractable Al and Fe

Average DCB extractable Fe and Al for the four representative samples were 2.36 ± 0.07 and 1.04 ± 0.04 wt%, respectively, while the AO extractable Fe and Al were 2.01 ± 0.08 and 1.71 ± 0.10, respectively (Table 1). These values fall within the range of extractable Fe and Al contents commonly measured in Podzols from a range of environments (Evans and Wilson, 1985; Sauer et al., 2007; Sauer et al., 2008). The DCB procedure removes Fe and associated Al from crystalline or non-crystalline oxides and oxyhydroxides, while the AO extraction removes Fe and Al present in non-crystalline oxide, oxyhydroxide and silicate phases. Thus, the ratio of AO-extractable Fe to DCB-extractable Fe, Fe_{AO}/Fe_{DCB}, provides an estimate of the fraction of Fe in non-crystalline phases. The Fe_{AO}/Fe_{DCB} ratios for our four soils ranged 0.80-0.92, indicating a preponderance of Fe in non-crystalline phases across all four samples (Table 1). Moreover, the ratio of AO-extractable Al to DCB-extractable Al, Al_{AO}/Al_{DCB}, indicated that there is almost twice as much Al in amorphous phases than in crystalline Fe oxides (Table 1).

SEM-EDS of the bulk soil

The thin section of the whole soil showed the existence of grains with sizes from ~10 mm across down to a very fine matrix (Figures 3, 4 and 5). Iron oxide was apparent as yellow-brown staining of different intensity in both the grains and the matrix (Figure 3a). The color suggested ferrihydrite or goethite, which is consistent with the results from extractable Fe that indicate that most Fe is in non-crystalline phases. Ferrihydrite is poorly crystalline and goethite can have very low crystal order (Kuhnel et al., 1975; Swayze et al., 2000). Some of the grains had a greenish color that suggested the existence of Fe^{2+} and thus of mineral grains that had not been sufficiently weathered to produce or complete Fe oxidation (Figure 3a). SEM showed a general structure of compound grains of heterogeneous composition hundreds of μm to ~1 mm in size and a loose collection of smaller grains and mineral matrix surrounding them (Figures 3b and 4a). The compound grains will be discussed later and are called clasts henceforth. Element mapping indicated quartz as the most abundant mineral and having a wide range of grain size (Figure 3c-h). Albite was also evident and

rather uniformly distributed between the clasts and loose grains (Figure 3e). Potassium was concentrated in K-feldspar (large grain in Figure 3f) and mica, also within and without the large clasts (Figure 3f). Iron concentrated in the clasts (Figure 3g), most probably as non-crystalline Fe oxides, forming rims near their edges (Figure 3a), making up part of the finest particles and accumulating in certain areas within the clasts (Figure 3g). Less frequently, Fe oxides were identified as discrete particles (Figure 4c). Magnesium was homogeneously distributed in the matrix and more abundant in specific grains such as those of chlorite and Mg-bearing mica (Figures 3h and 4b). Mica grains had a large range of particle size and Mg content (Figure 4b and corresponding spectra). The most homogeneously distributed of all elements was Al, present in all mineral grains except quartz (Figure 3d).

The very fine matrix within the large clasts could be observed as featureless areas between distinct grains, containing Si, Al, Fe, K, Mg and very little Na and Ti (spectrum 2 in Figure 4d; Cl and P are from the Epoxi resin). Figure 5 is a detail of the texture of the small mineral grains next to a larger grain, all of them within a clast. The back-scattered electron image (Figure 5a) shows small particles with light contrast, as coatings or precipitates between other particles. Most of them are probably Fe oxides although there might be also other oxides, such as Ti and Mn oxides. The secondary electron image (Figure 5b) revealed the texture of the particles within the clast, showing the presence of irregular grains (quartz, feldspars), many of them with corrosion signs, plates of different size (phyllosilicates), and areas of indistinct morphology (fine matrix). Particularly remarkable is the large round grain at the left, bottom corner of the image (Figure 5). This grain is of inorganic composition as indicated by the contrast in back-scattered electrons (an organic composition would produce a darker contrast than that of the surrounding grains) and seems to be an aggregate of very small particles that cannot be resolved in the image.

SEM-EDS of the < 2 μm size fraction

The very fine material was investigated in more detail in the < 2 μm size fraction by sedimenting this material from water dispersions. This material appeared as particles < 1 μm (Figure 6) with no defined morphology. The composition of these particles was investigated in individual point analyses and analyses of areas (a few μm to ~ 30 μm by side), but in every case many grains were analyzed given their small particle size. The composition of these particles was variable but can be defined as that of a silicate with Si > Al >> Fe, Mg, K, Na (Figure 6, spectra 1,b; 1,c; 1,d). Iron was higher in other collected spectra not shown here. Larger particles, corresponding to the mineralogy found using XRD, were thinly distributed on the non-crystalline grains. The most abundant grains were quartz, typically with clear signs of alteration both chemical and morphological (not shown). Some examples of large grains are shown in Figure 6, corresponding to the phyllosilicates identified using XRD.

Soil chemistry from EDS

All the EDS results from the thin section (whole soil) and sediments (fraction < 2 μm, with and without previous Al and Fe extraction with AO) were used to construct plots that provided a global view of the composition of the soil (Figure 7). The results were expressed as atomic ratios. These plots show the presence of Fe, Al, Na, K and Mg in quartz grains; of Fe, K and Mg in plagioclase and, particularly, albite; and of Fe and Na in K-feldspar. In kaolinite grains there was Fe, K, Na and Mg, and some of the chlorite grains showed K (Figure 7c). These results could be due to (1) contamination of the analyses from other mineral grains and/or (2) alteration of the analyzed grains. Given the typical large size of the analyzed individual grains (Figures 3, 4 and 6) and the assessed analyzed volume (diameter at the surface of < 200 nm; depth 1-3 μm) we believe that there are cases of real chemical alteration of the individual grains. This is supported by the signs of corrosion and alteration observed in individual grains (Figures 4-6). For this reason, we label the analyses with elements alien to the mineral phase as “altered” (Figure 7). Certainly, kaolinite in soils frequently contains Fe (Ryan and Huertas, 2009). In some of the plots (Figure 7a,c), altered

kaolinite particles plot very close to muscovite particles, however the interpretation of their kaolinitic nature is based on the absence or low K content (Figure 7b; data points with no K are not represented).

Chlorite presented a range of Al/Si and Fe/Si ratios both ranging within 0.1-2 (Figure 7a), which suggests substitution between Al and Fe. Magnesium was also present (Figure 7c) with a narrower range of Mg/Si ratios (not shown in the plots) of 0.35-0.97. Muscovite had a range of Fe and Mg contents, although we suspect that muscovite grains with Fe/Si close to 1 or above were altered or had Fe oxide coatings. The latter must be the case when Al/Si was also ~1 (Figure 7a). Muscovite had small amounts of Mg (Figure 7c) with Mg/Si ranging 0-0.08 (not shown). A few analyses represented metal oxides mixed with silicate phases, and they are characterized by Fe/Si ratios > 10 and Al/Si ratios > 1.8 (Figure 7a,c).

Three element maps were collected (Figure 3 and two similar ones) and the average composition of the entire area measured (187,500-750,000 μm^2) is very similar, with the exception of the K/Mg ratio (Figure 7). The corresponding cation ratios can be considered an approximation to those in the bulk soil. The multiple analyses of areas on the very fine matrix from the sedimented size fraction < 2 μm (termed “background” in Figure 7) gather mainly around narrow margins of metal ratios, with a minority of data points having a dispersed distribution. These values of the fine matrix include samples for which Al and Fe was extracted with AO (red “background” symbols in Figure 7). Both data sets (with and without Al and Fe extraction) had the same distribution, indicating that most of the fine matrix was not solubilized with AO. The areas of maximum concentration of data points from the fine matrix in each plot are close to the composition of the bulk soil, with only slightly higher Al/Si and K/Si ratios (Figure 7). The Fe/Si vs. Al/Si ratios of the fine matrix without the area of data point concentration fall mainly in the ranges of composition of mica and chlorite (Figure 7a).

DISCUSSION

Soil fabric

Soil from the B/C horizon contained mm-size clasts and loose grains of a very large range of particle size (Figure 3). When observed in detail, the particles in the large clasts were not cohesively bound, but had mineral grains with a large size range and distributed randomly in terms of size and orientation, although local orientation of elongated particles could be observed in some places (Figure 5). At the border of the clasts, the particles were approximately oriented with their longest dimension parallel to the edge (Figures 3, 4a, 5). There was a slight difference in contrast between this external edge and the rest of the clast (Figures 3, 4a, 5) suggesting that the particles at the edge were attached during pedogenesis (i.e., these particles were not originally in the clasts). This different contrast (slightly darker) may be due to a combination of lower amount of Fe oxides (Fe oxides appear brighter in back-scattered electron images), lower density of mineral grains, and the inclusion of organic matter (Figures 3, 4). However, the darker contrast in the edges was not always apparent (Figure 5). In some areas, the edge contained a very high proportion of the fine matrix (Figure 5).

The minerals in the clasts (quartz, plagioclase, feldspar, muscovite, chlorite and kaolinite; Figures 2, 3 and 4) are all typical of sandstone (e.g., Worden and Burley, 2003) and the chlorite composition matches a common range in sandstones, where Fe and/or Al are more abundant than Mg (Figure 7; Weaver, 1989). The fabric of the clasts is also compatible with the soil deriving from sandstone (Figures 3, 4a).

Podzols generally have a sandy texture, lacking sufficient clay to produce well-formed aggregates. However, where discernible aggregation occurs, the leached E horizon is commonly granular while the underlying B horizons vary from subangular blocky to very hard and massive. Furthermore, due

to their coarse texture, Podzols are usually well drained and may experience drought conditions even in regions of high rainfall. If drainage is restricted, however, the Bs horizon may become weakly and irregularly cemented leading to formation of a hardpan or, where the cementation is continuous, an ortstein layer (Wang et al., 1978). The cemented layer grades downward into the altered parent material (B/C). In our soils, the discrete clasts were not translocated from the upper horizons as indicated by their large size. Rather, they were most likely present in the sandstone and underwent alteration in situ throughout their volume. This would explain the corrosion observed in quartz, feldspar and plagioclase grains within the clasts (Figure 5) and the possible signs of mineral alteration found in the chemical data (Figure 7). The loose grains outside the clasts (Figures 3, 4), could correspond to particles transported downwards (eluviation) and to particles in former clasts that were totally dispersed in situ during the weathering process. The clasts accreted some of these grains around them during pedogenesis, that remain attached to the clasts with a preferential orientation parallel to the surface of the clasts (Figure 5). In some cases it is difficult to assess whether some particle aggregates were inherited from the sandstone or pedogenic, as that in the center of Figure 4b. We interpret that the small size of this aggregate, the large amount of undifferentiated matrix and the low density of the packing of the grains suggest that this and similar cases correspond to aggregates generated during incipient soil formation. The precipitation of secondary phases may have contributed to aggregation, as many grains displayed rims of Fe oxides (Figure 3a).

It can be questioned that the studied soil formed on the original sandstone rock because there is evidence of solifluction (Clark et al., 1998) and wind deposits (Clark and Wilson, 1992; Wilson, 1994) in the Falklands. The soil could have developed on the head or sand deposits produced by solifluction and wind transport. A sheet of periglacial mass movement deposits is mapped across the centre of East Falkland extending to within 4.1 km north of the study site but the area of the studied soil lacks such deposits, and the surface material is described as corresponding to the

underlying Fitzroy Tillite formation (Falkland Islands Renewable Energy web project, 2016). Soil development on transported masses can then be discarded. Podzol formation on wind-deposited sands has taken place in the Falklands (Wilson, 2001). However, the presence of cm-size fragments (Appendix Figure A.2) and of 5-10 mm clasts (Figure 3a) in the studied soil are incompatible with aeolian transport.

Chemical weathering process

The most interesting characteristic of our Podzol is the generation of a large proportion of very fine particles (< 1 μm, Figure 6) with a composition similar to an Al-Fe rich smectite (Figures 4d, 6b,c,d) that do not diffract X-rays (Figure 2). The composition appears fairly uniform (Figure 7), although this uniformity may be due to the fact that most of the analyses included multiple particles (EDS analysis of areas several to tens of μm on each side; see methods). We propose that these solids form partly through the effects of podzolisation, the multifarious physicochemical processes producing the downward migration of, principally, Al- and Fe-organic matter complexes, followed by the subsequent precipitation of these organo-metallic chelates in the spodic horizon and below. Additionally, colloidal gels formed in the upper soil may be transported down the profile with the percolating waters. A reduced hydraulic conductivity in the B/C horizon will facilitate accumulation of solutes and gels. The in situ alteration of the primary minerals in the B/C horizon also contributes to the precipitated gels, as indicated by signs of corrosion in the mineral grains (Figure 5).

The composition of the fine matrix is close to that of the bulk soil as obtained from the average composition of large areas (187,500-750,000 μm^2) of the soil thin section (Figure 7). There are two possible reasons for this observation that are not mutually exclusive. First, that the fine matrix makes up most of the bulk of the soil. However, the SEM images suggest that the maximum matrix content in the observed area of the soil thin section is perhaps 50% (Figures 3, 4, 5). Second, that the fine matrix is the result of precipitation of solutes contributed by minerals proportionally to their

abundance, in which case the precipitates would have a composition similar to the bulk soil. The solutes from which the precipitates formed are probably both translocated from the horizons above and generated by dissolution in the B/C horizon. It is impossible that the non-crystalline matrix contains material that has not been dissolved and precipitated in the soil because (1) the soil derives entirely from sandstone and (2) sandstone contains only crystalline mineral phases. It may seem strange that minerals with different solubility, such as quartz and albite, to mention the two most abundant minerals, may contribute similarly (always in proportion to their abundance) to the alteration products. However it should be considered that the absolute surface exposed to solution of each primary mineral is approximately proportional to its abundance in the soil. For each specific mineral, the larger the exposed surface the larger its contribution to the dissolved species in the interstitial fluids. It is also necessary that the water was rather immobile at the base of the illuvial horizon, became saturated and the newly formed gels contained approximately the same cations that were dissolved from the original minerals. In other words, the most mobile ions, such as Na or Mg, could not be transported away because of the low hydraulic conductivity. One conclusion is, then, that the alteration process took place in a rock-dominated system. Podzol formation requires vertical movement of water in order to develop the E and podzolic B horizon, but these horizons were eroded in our soil. The only existing horizon was the B/C, which is frequently poorly drained or waterlogged in the Falklands Podzols (Cruickshank, 2001).

The soil is derived from the sandstone in the Fitzroy Tillite formation. These rocks are Carboniferous to Permian in age (350-250 Ma; Aldiss and Edwards, 1999). The investigated soil must have started its development at some unknown time after the end of the last glaciation (14 Ka BP). Previous soils or sediments were eroded by periglacial processes or by winds. Indeed, winds are most effective erosion agents in cold climates that do not support large vegetation mass. This would be in agreement with the evidence of ventifacts aged 11-13.6 Ka generated after a period of severe cold (Clark and Wilson, 1992). Wilson (2001) described Podzol formation in sands in the

Falklands, developed in periods ranging 300-500 a to 2500-3000 a, depending on the drainage conditions of the sands (better drained sands took longer to develop soils) and probably on the climate (a later, wetter climate developed soils faster). The speed of podzolization in our site was most probably slower than those described by Wilson (2001) because it started with the solid tillite, rather than sands.

We observe little alteration at the base of our Podzol, as expected. The fabric of the parent material is still preserved in large grains (the "clasts" discussed above), while from the chemical and mineralogical point of view there is a good preservation of mineral grains from the original sandstone, including albite, mica of different Al-Mg-Fe composition and chlorite (Figures 3, 4, 6, 7). More importantly, the alteration products are not crystalline. The two obvious alteration products are the Fe oxides and the fine silicate matrix. The greatest part of the Fe oxides are not crystalline as indicated by the fact that most free Fe was extracted with the AO method (Table 1) and because no Fe oxides were observed in XRD patterns (Figure 2). The fine matrix is not crystalline either because it is not observable with XRD. The lack of non-crystalline alteration products indicates that the crystallization of the gels in the B/C horizon, and perhaps also in the Bs horizon above, was arrested. The most likely reason for such phenomenon is weathering in the B horizons taking place with low water/rock ratio or with low water mobility, producing rapid fluid saturation, gel precipitation and the arrest of gel crystallization. Podzolization requires sufficient precipitation to mobilize Fe and Al from the top horizons, and peat formation in the O horizon requires waterlogging. Accordingly, an equilibrium between precipitation and evaporation may have existed to allow sufficient leaching of the E horizon and low water/rock ratio or hydraulic conductivity in the B horizons. Water infiltrating the B/C horizon, perhaps also the Bs, may have been short-lived or insufficient to transport weathered cations away from these horizons. Reduced water activity and water evaporation may have been produced by freezing temperatures and high winds, respectively. Present annual precipitation in the area where the investigated soil was

collected is low at ~550 mm and there are frequent strong winds and occasional frosts (Jones et al. 2013; McAdam, 2013, 2014). All these climate characteristics are compatible with a reduced mobility of water in the B horizons of the developing Podzol.

The existence of the fine matrix with a smectite-like composition and no detectable crystal structure is a rare phenomenon. It can be discarded that this material is related to extractable Al or Fe in non-crystalline phases because the extraction with AO caused no appreciable difference in the amount of fine matrix that was collected in the < 2 μm size fraction and no apparent changes in the composition of this matrix (Figure 7). In other words, although the matrix is not crystalline it cannot be solubilized with AO. This indicates that the fine matrix does not have a significant component of allophane or imogolite, both of which are dissolved with the AO method (Smith, 1994). We investigated whether the matrix had a homogeneous composition. Portions of the fine matrix have Fe/Si versus Al/Si ratios very similar to those of chlorite and mica (Figure 7a). Similarly, there are data points of K/Mg vs Al/Si coincident with those of mica (Figure 7c), K/Si ratios in the range of mica, and Na/Si ratios in the range of albite data points (Figure 7b). It may be the case that some of these gels were precipitated in the proximity of grains of the above minerals that were undergoing dissolution and, due to the low water mobility, the composition of the gel particles mimics that of the dissolving mineral grains. The great majority of the data points that accumulated within narrow ranges in plots of metal ratios (Figure 7) were from chemical analyses of areas covering many grains in the samples prepared as sediments (< 2 μm fraction). These samples had been dispersed in water and thus their grains were redistributed. On the contrary, few analyses of individual matrix particles in the thin section were within the highly concentrated areas in the chemical plots. Specifically, only 6-15% of particles from the thin section were within the values that bracket the most frequent ratios (Al/Si = 0.45-0.6; Fe/Si = 0.3-1.2; K/Si = 0.07-0.12; Na/Si = 0.015-0.035; K/Mg = 1-2.5), whereas 50-82% of the measurements from the sediment (< 2 μm) were within these ranges. This indicates that individual grains of the fine matrix have heterogeneous

composition. One factor that would have contributed to such a situation is the hypothesis that precipitation occurred near dissolving particles and thus the corresponding grains in the fine matrix preserved to a variable extent the composition of the dissolved particles. Solutes translocated from the above horizons may have also precipitated gel particles of heterogeneous composition in a system with little water mobility.

As the altering fluids soon became solute-rich, it would be expected that the alteration product was smectite, the typical product in poorly drained systems (Chamley, 1989). We therefore investigated the possibility that the non-crystalline matrix had an average composition similar to smectite. The composition from all analyses of the fine matrix was averaged and recalculated as if it was a phyllosilicate, which yielded the following composition: ($Si_{2.70}$ $Al_{1.30}$) ($Al_{0.19}$ $Mg_{0.15}$ $Fe_{1.95}$ $Ti_{0.05}$) $Na_{0.11}$ $K_{0.26}$ per 22 negative charges, that would correspond to an interlayer charge of 0.36 and a total octahedral content of 2.34 atoms. This formula does not represent a real mineral phase but rather indicates that the average composition of the matrix approaches that of a dioctahedral smectite. The most obvious difference is that the octahedral content is high and the Si content low, both of which would result from excessive Al+Fe, which is expected in a Podzol, where Fe and Al are translocated from above horizons. It can be interpreted that the fine matrix, loose or interspersed between mineral grains in the clasts, is a gel that would eventually generate dioctahedral smectite of variable composition plus some other minor (Al- and/or Fe-rich) phases.

The existence of a macroscopic, abundant and non-extractable (insoluble to usual methods for extraction of poorly ordered phases), non-crystalline silicate phase, apparently precursor of the secondary phase(s) caused by weathering, is a very rare phenomenon. According to our knowledge, the most similar case was described by McKeague and Brydon (1970), who identified an amorphous silicate phase with XRD (large background increase between 20 and 40 °2θ) in two Podzols from Nova Scotia and New Brunswick, Canada, in Bf horizons where chlorite had been

entirely dissolved. One of these soils was imperfectly drained and the other well drained. McKeague and Brydon (1970) did not investigate the composition of this amorphous component or its solubility. There is then a coincidence with our study in the type of soil and the horizon where the amorphous phase was found. The present climate for the Canadian Podzol is also similar to that for our Falklands soil, with minimum yearly average temperatures ranging between -7 and -9 °C and maxima of 20 °C, and with average precipitation of 1080 mm (New Brunswick) and 1038 mm (Nova Scotia; Environmental Canada, 2016). Thus, the Canadian soils experienced more precipitation than the one in the Falklands, but also lower, freezing temperatures, that would reduce water activity.

The following case described the dissolution of a mineral phase in a Podzol without the appearance of any recognizable secondary phase, which might suggest the formation of non-crystalline phases difficult to observe. Bain (1977) described the dissolution of ferruginous chlorite in the eluvial horizon (A_2 horizon as described by Bain, 1977, using Glentworth and Muir, 1963) of a Podzol in Scotland, where the only apparent secondary phase was goethite. The soil was described by Bain (1977) as a Podzol with a thin humus iron pan and free draining. Bain (1977) did not detect any extractable Si and Al amounts that could account for the missing chlorite, which was abundant in other horizons of the soil profile. Present average monthly temperatures in Argyllshire range 4-12 °C, and the total annual average precipitation is 1,700 mm (Met Office, 2016). Thus, in Argyllshire, the temperature range is similar to that in the Falklands location (2-9 °C) but the climate is much more humid (~550 mm in the Falklands location) and the soil drainage is good. Thus the condition of a low water/rock ratio for the precipitation of an amorphous gel during weathering does not apply to the Argyllshire site and total removal of much of the elements making up the chlorite is possible.

Kodama and Brydon (1968) described the mineralogy of other Podzols in New Brunswick, where chlorite had disappeared from Ae horizons. Here the authors interpreted that the dissolved chlorite

left an amorphous silicate residue, not based on direct evidence but on previous results from chlorite dissolution in acidic conditions. Mitchell and Farmer (1962) found large amounts of non-crystalline silicate material in the A and C horizons of Scottish soils (the only two horizons studied) of variable composition, with an average atomic ratio of Si:Al:Fe of 3.9:2.8:1.0. The material was extracted with Na carbonate and DCB treatments. The ranges of soluble silica and alumina in the soil horizons were 72-86% and 43-58% of the total silica and alumina, respectively. Mitchell and Farmer (1962) called this material "allophane", but the use of this name was not as precise then as it is now. Similarly, Loveland and Bullock (1976) investigated the amorphous components of brown podzolic soils and found, in some cases, relatively large proportions of extractable Fe, Al and Si (up to 6%), some of them characterized by them as allophane. Loveland and Bullock (1976) did not mention non-extractable amorphous material. Amorphous coatings on mineral particles were described by McKyes et al. (1974) making up to 12 wt% of clay soils from Quebec, Canada. The amorphous coatings consisted mainly of SiO_2 and Fe_2O_3 with a small proportion of Al_2O_3. The amorphous phase was extracted by successive treatments at low and high pH (8 N HCl and 0.5 N NaOH solutions, respectively). McKyes et al. (1974) interpreted that this phase was not a silicate gel but a combination of Fe oxide or hydroxide and silica, with chemisorption of one phase onto the other.

Given the rarity of the phenomenon described here it is worth investigating whether any similar situations have been found in systems other than soils. To our knowledge, the most similar example is that described by Cuadros et al. (2011), who found gels from submarine hydrothermal sediments with particles with a smectite-like, heterogeneous composition that produced very weak and imperfect electron diffraction patterns and HRTEM lattice fringes of 10-15 Å. A few wide XRD peaks could possibly be assigned to a smectite phase of low crystallinity. These gels were interpreted by Cuadros et al. (2011) as proto-smectite that had acquired chemical and micro-morphological characteristics of smectite but without the complete crystal structure.

There are multiple descriptions of poorly crystalline intermediates in the formation of smectite in soils and other environments but they differ from our study in that abundant smectite observable with XRD was already formed and that the intermediate phases were only present at a microscopic scale. Singh and Gilkes (1993), using SEM and TEM, observed a poorly crystalline intermediate between pyroxene and smectite in the weathered rock at the bottom of one profile in lateritic soils. Banfield and Eggleton (1990) identified a poorly crystalline intermediate between feldspar and smectite in weathered granodiorite, using TEM. In this case, there is no information about how much smectite was already present. Charpentier et al. (2011) found Fe-rich montmorillonite forming from gels in deep-see sediments. The gels were interpreted to be generated by the dissolution of volcanic glass, siliceous fossils, silicates and pyrite oxidation. Steep chemical gradients could be observed at TEM resolution (< 1 μm) between the amorphous phases and the crystallized smectite. Giorgetti et al. (2009) found that low-temperature (< ~150 °C) hydrothermal alteration of trachybasalt generated smectite of variable composition, depending on the altered mineral phase. Alteration of crystalline phases (pyroxene, plagioclase, biotite) produced crystalline smectite with no observable intermediate. Alteration of volcanic glass also produced smectite, but in this case associated with an intermediate semicrystalline phase (d-spacing of 3 Å) and a poorly crystalline smectite (10 Å d-spacing) (both observed with HRTEM). In this case smectite was also abundant and observed with XRD. Giorgetti et al. (2009) suggested that the transformation of the volcanic glass into smectite through an intermediate of progressively increasing crystallinity is due to low water/rock conditions caused by low rock permeability. It is interesting that Giorgetti et al. (2009) found no protocrystalline intermediates between crystalline phases and smectite, even though they were weathered presumably under the same water/rock regime. Formation of allophane and imogolite in volcanic soils that evolve towards smectite with increasing weathering is well-known (Chamley, 1989) and protocrystalline intermediates during the formation of clay from silicate glass and gels of different origin and composition have been found frequently (e.g., Tazaki

et al., 1989; Stroncik and Schmincke, 2001; Huertas et al., 2004). However, the process investigated in our soil is different because the gels in the soil were generated from the dissolution of preexisting minerals during weathering, whereas, in these other studies, the glass was one or the only original mineral phase being weathered.

In conclusion, the gels in the Falklands soil are different from so many others that have been described in the literature because they combine the following characteristics: (1) they make up a large amount of the soil, (2) they are insoluble by the usual methods of extraction of non-crystalline phases, and (3) they are the only secondary phase generated by weathering (i.e., no secondary crystalline phases exist).

We suggest that the low crystallinity of the Fe oxides in the soil (possibly ferrihydrite or goethite, according to the color) is due also to the low mobility of water during weathering (perhaps including low water/rock ratio conditions) that cause (1) fast saturation and precipitation, and (2) very slow crystallization kinetics of the precipitated non-crystalline phase. The Fe and Al extractable with AO were not detected to be concentrated in the < 2 μm size fraction, for which reason it can be assumed that they were distributed in the bulk soil both as coating on large grains and dispersed in the finer fraction. This is probably the case also for Fe oxide phases with associated Al extracted with DCB (Table 1). All these compounds appear as yellow-brown, depending on their concentration, and they can be seen as rims of grains and in the fine fraction of the soil (Figure 3a), as well as within the mineral grains described as clasts (Figures 3c,g and 4a,c).

IMPLICATIONS

This study provides evidence of a weathering processes taking a yet unknown route. Low water mobility and water/rock ratio are considered the cause of the exceptionally slow weathering process taking place in the investigated soil, which has resulted in the formation of a gel sufficiently stable

to resist extraction with methods for non-crystalline phases but with no development of a crystal structure. Is this a very restricted phenomenon or does it take place frequently in places where climatic conditions restrict water activity? Such places could be high latitude or semiarid environments, or those where high winds, as in the Falklands, reduce soil moisture. The typical weathering process described for cold and arid environments is the physical disaggregation of the rock, with large preservation of the original mineralogy. The same process is found in our Falklands soil from the Fitzroy area, except for the large silicate gel content that is accounted for by the higher temperature and precipitation (the climate in the Falklands is not arid or cold). Are studies of similar soils, particularly of their lower horizons, missing the existence of a substantial proportion of a silicate gel, not observable in XRD or extraction investigations? If the existence of this intermediate gel is relatively frequent, our finding will open the possibility of studying weathering reactions with great detail, as the process takes place “at slow motion”. Further studies of similar soils may show how the gel evolves, as it interacts with the fluids and parent minerals, into the formation of crystalline phases, presumably consisting mainly of smectite. These soils where weathering is slow may be an exceptional laboratory to show the several processes and steps that are bypassed or too fast to be observed during weathering in soils everywhere else.

ACKNOWLEDGMENTS

We thank Alan Eagle to allow sampling in his farm, Dr. Emma Humphreys-Williams for help with the C-N analyses, and Dr. Tobias Salge for help with the SEM-EDS investigation. A.D. was funded by the Falkland Islands Government Environmental Studies Budget, project 'Establishing the Falkland Islands Native Seed Hub for habitat restoration' (July-December 2013). S.W.S. was funded by Darwin Plus Initiative Project (DPLUS023) via Department of Environment, Food and Rural Affairs, UK and Shackleton Scholarship Fund (2015/2016). The Earth Sciences Department of the Natural History Museum funded the analytical work and M.C.

REFERENCES CITED

Adie, R.J. (1952b) Representatives of the Gondwana System in the Falkland Islands. Symposium sur les series de Gondwana, XIXth International Geological Congress, Algiers, pp. 385-392.

Aldiss, D.T., and Edwards, E. J. (1999) The geology of the Falkland Islands. British Geological Survey Technical Report WC//10.

Anderson, S.P., Blanckenburg, F., and White, A.F. (2007) Physical and chemical controls on the Critical Zone. Elements, 3, 315-319.

Bain, D.C. (1977) The weathering of ferruginous chlorite in a Podzol from Argyllshire, Scotland. Geoderma, 17, 193-208.

Banfield, J., and Eggleton, R. (1990) Analytical transmission electron microscopy studies of plagioclase, muscovite, and K-feldspar weathering. Clays and Clay Minerals, 38, 77-89.

Buurman, P., and Jongmans, A.G. (2005) Podzolisation and soil organic matter dynamics. Geoderma, 125, 71 - 83.

Chamley, H. (1989) Clay Sedimentology. Springer-Verlag, Berlin.

Charpentier, D., Buatier, M.D., Jacquot, E., Gaudin, A., and Wheat, C.G. (2011) Conditions and mechanism for the formation of iron-rich montmorillonite in deep sea sediments (Costa Rica margin): Coupling high resolution mineralogical characterization and geochemical modeling. Geochimica et Cosmochimica Acta, 75, 1397-1410.

Chorover, J., Kretzschmar, R., Garcia-Pichel, F., and Sparks, D. (2007) Soil biogeochemical processes within the Critical Zone. Elements, 3, 321-326.

Clapperton, C.M. (1971) Evidence of cirque glaciation in the Falkland Islands. Journal of Glaciology, 10, 121–125.

Clark, R. (1972) Periglacial landforms and landscapes in the Falkland Islands. Biuletyn Peryglacjalny, 21, 33–50.

Clark, R. (1976) Further consideration of Falkland Islands periglacial landscapes. Biuletyn Peryglacjalny, 26, 167–174.

Clark, R., and Wilson, P. (1992) Occurrence and significance of ventifacts in the Falkland Islands, South Atlantic. Geografiska Annaler, 74A, 35–46.

Clark, R., Huber, U.M., and Wilson, P. (1998) Late Pleistocene sediments and environmental change at Plaza Creek, Falkland Islands, South Atlantic. Journal of Quaternary Science, 13, 95–105.

Climate-Data.org (2016) http://en.climate-data.org/country/78/ (accessed 13.11.16).

Cruickshank, J.G. (2001) Falkland Soils – origins and prospects. Unpublished Report to the Department of Agriculture, Stanley. Department of Agriculture for Northern Ireland, Belfast.

Cuadros, J., Dekov, V.M., Arroyo, X., and Nieto, F. (2011) Smectite formation in submarine hydrothermal sediments: samples from the HMS Challenger expedition (1872-1876). Clays and Clay Minerals, 59, 147-164. doi 10.1346/CCMN.2011.0590204

Drouin, D., Réal Couture, A., Gauvin, R., Hovington, P., Horny, P., and Demers, H. (2001) CASINO: monte CArlo SImulation of electroN trajectory in sOlids, version 2.42. University of Sherbrooke, Canada.

Drouin, D., Réal Couture, A., Joly, D., Tastet, X., Aimez, V., and Gauvin, R. (2007) CASINO V2.42—A fast and easy-to-use modeling tool for scanning electron microscopy and microanalysis users. Scanning, 29, 92-101.

Egli, M., Zanelli, R., Kahr, G., Mirabella, A., and Fitze, P. (2002) Soil evolution and development of the clay mineral assemblages of a Podzol and a Cambisol in 'Meggerwald', Switzerland. Clay Minerals, 37, 351-366.

Environmental Canada (2016) Meteorological Service of Canada. Canadian Climate Normals. 1981-2010 Climate Normals & Averages. http://climate.weather.gc.ca/climate_normals/index_e.html (accessed, 13.11.16).

Evans, L.J., and Cameron, B.H. (1985) Color as a criterion for the recognition of podzolic B horizons. Canadian Journal of Soil Science, 65, 363-370.

Evans, L.J., and Wilson, W.G. (1985) Extractable Fe, Al, Si and C in B horizons of podzolic and brunisolic soils from Ontario. Canadian Journal of Soil Science, 65, 489-496.

Falkland Islands Renewable Energy web project (2016) http://148.251.4.143/saeri_lm3beta3/lizmap/www/index.php/view/map/?repository=v02&project=renewable_energy (accessed 8.12.16).

Giorgetti G., Monecke T., Kleeberg R., and Hannington M. (2009) Low-temperature hydrothermal alteration of Trachybasalt at Conical Samount, Papua New Guinea: formation of smectite and metastable precursor phases. Clays and Clay Minerals, 57, 725-741.

Glentworth, R., and Muir, J.W. (1963) The soils of the country around Aberdeen, Inverurie and Fraserburgh. H.M. Stationery Office, London.

Hansom, J.D., Evans, D.J.A., Sanderson, D.C.W., Bingham, R.G., and Bentley, M.J. (2008) Constraining the age and formation of stone runs in the Falkland Islands using Optically Stimulated Luminescence. Geomorphology, 94, 117–130.

Hodgson, D.A., Graham, A.G.C., Roberts, S.J., Bentley, M.J., Ó Cofaigh, C., Verleyen, E., Vyverman, W., Jomelli, V., Favier, V., Brunstein, D., Verfaillie, D., Colhoun, E.A., Saunders, K.M., Selkirk, P.M., Mackintosh, A., Hedding, D.W., Nel, W., Hall, K., McGlone, M.S., van der Putten, N., Dickens, W.A., and Smith, J.A. (2014) Terrestrial and submarine evidence for the extent and timing of the Last Glacial Maximum and the onset of deglaciation on the maritime-Antarctic and sub-Antarctic islands. Quaternary Science Review, 89, 129–147.

Huertas F.J., Fiore S., and Linares J. (2004) In situ transformation of amorphous gels into spherical aggregates of kaolinite: A HRTEM study. Clay Minerals, 39, 423-431.

IUSS Working Group WRB. (2015) World Reference Base for Soil Resources 2014, update 2015 International soil classification system for naming soils and creating legends for soil maps. World Soil Resources Reports No. 106. FAO, Rome.

Jones, P.D., Harpham, C., and Lister, D.H. (2013) Construction of high spatial resolution climate scenarios for the Falkland Islands and southern Patagonia. United Kingdom Falkland Islands Trust. http://www.ukfit.org/wp-content/uploads/2014/08/FALKLANDS-CLIMATE-CHANGE_report_08-10-2013.pdf (accessed 25.04.16).

Kodama, H., and Brydon J.E. (1968) A study of clay minerals in podzol soils in New Brunswick, Eastern Canada. Clay Minerals, 7, 295-309.

Konhauser, K.O., Fyfe, W.S., Ferris, F.G., and Beveridge, T.J. (1993) Metal sorption and mineral precipitation by bacteria in two Amazonian river systems: Rio Solimoes and Rio Negro, Brazil. Geology, 21, 1103-1106.

Kuhnel, R.A., Roorda, H.J., and Steensma J.J.(1975) The crystallinity of minerals; a new variable in pedogenetic processes; a study of goethite and associated silicates in laterites. Clays and Clay Minerals, 23, 349-354.

Loveland, P.J., and Bullock, P. (1976) Chemical and mineralogical properties of brown podzolic soils in comparison with soils of other groups. Journal of Soil Science, 27, 523–540.

McAdam, J.H. (2013) The impact of the Falklands War (1982) on the peatland ecosystem of the Islands. In: I.D. Rotherham and C. Handley, Eds., War and Peat, pp. 143-162. Wildtrack Publishing, Sheffield, UK.

McAdam, J.H. (2014) Farming on the peatlands of the Falkland Islands. http://www.ukfit.org/wp-content/uploads/2014/08/MCADAM-FARMING-ON-FALKLANDS-PEATLANDS-FINAL-VERSION2-TO-SHEFFIELD.pdf (accessed 20.11.16).

McKeague, J.A., and Brydon, J.E. (1970) Mineralogical properties of ten reddish brown soils from the Atlantic provinces in relation to parent materials and pedogenesis. Canadian Journal of Soil Science, 50, 47-55.

McKeague, J.A., De Coninck, F., and Franzmeier, D.P. (1983) Spodosols. In, L.P. Wilding, N.E. Smeck, and G.F. Hall, Eds., Pedogenesis and Soil Taxonomy, II. The soil orders, pp. 217-252. Elsevier, New York, USA and Amsterdam, The Netherlands.

McKyes, E., Sethi, A., and Yong, R.N. (1974) Amorphous coatings on particles of sensitive clay soils. Clays and Clay Minerals, 22, 427-433.

Met Office (2016) Meteorological Office of the UK. Data from 1981 to 2010. http://www.metoffice.gov.uk/public/weather/climate (accessed 15.11.16).

Mitchell, B.D., and Farmer, V.C. (1962) Amorphous clay minerals in some Scottish soil profiles. Clay Minerals Bulletin, 2, 128-144.

Ryan, P.C., and Huertas, F.J. (2009) The temporal evolution of pedogenic Fe-smectite to Fe-kaolin via interstratified kaolin-smectite in a moist tropical soil chronosequence. Geoderma, 151, 1-15.

Saccone, L., Conley, D., Likens, G., Bailey, S., Buso, D., and Johnson, C. (2008) Factors that control the range and variability of amorphous silica in soils in the Hubbard Brook Experimental Forest. Soil Science Society of America Journal, 72, 1637–1644.

Sauer, D., Sponagel, H., Sommer, M., Giani, L., Jahn, R., and Stahr1, K. (2007) Podzol: Soil of the Year 2007, A review on its genesis, occurrence, and functions. Journal of Plant Nutrition and Soil Science, 170, 1–17.

Sauer, D., Schülli-Maurer, I., Sperstad, R., Sørensen, R., and Stahr, K. (2008) Podzol development with time in sandy beach deposits in southern Norway. Journal of Plant Nutrition and Soil Science, 171, 483–497.

Shang, C., and Zelazny, L.W. (2008) Selective dissolution techniques for mineral analysis of soils and sediments. In: A.L. Ulery, and L.R. Drees, Eds., Methods of Soil Analysis, Part 5. Mineralogical Methods, pp. 33–80. Soil Science Society of America Book Series, Madison, Wisconsin, USA.

Singh, B., and Gilkes, R.J. (1993) Weathering of spodumene to smectite in a lateritic environment. Clays and Clay Minerals, 41, 624-630.

Smith, B.F.L. (1994) Characterization of poorly ordered minerals by selective chemical methods. In: M.J. Wilson, Ed., Clay Mineralogy: Spectroscopic and Chemical Determinative Methods, pp. 333-357. Chapman and Hall, London, UK.

Stone, P. (2011) Borehole core recovered from the Late Carboniferous to early Permian Fitzroy tillite and Port Sussex formations, Falkland Islands: geological background and sample details.

British Geological Survey, Open Report OR/11/028. http://nora.nerc.ac.uk/14415/1/OR11028.pdf (accessed 23.10.16).

Stone, P., Thomson, M.R.A., and Rushton, A.V. (2012) An Early Cambrian archaeocyath-trilobite fauna in limestone erratics from the Upper Carboniferous Fitzroy Tillite Formation, Falkland Islands. Earth and Environmental Science Transactions of the Royal Society of Edinburgh, 102, 201-225.

Stroncik, N.A., and Schmincke, H.U. (2001) Evolution of palagonite: Crystallization, chemical changes, and element budget. Geochemistry Geophysics Geosystems, 2, 2000GC000102.

Swayze, G.A., Smith, K.S., Clark, R.G., Sutley, S.J., Pearson, R.M., Vance, J.S., Hageman. P.L., Briggs, P.H., Meier, A.L., Singleton, M.J., and Roth, S. (2000) Using imaging spectroscopy to map acidic mine waste. Environmental Science and Technology, 34, 47-54.

Tazaki, K., Fyfe, W., and van der Gaast, S. (1989) Growth of clay minerals in natural and synthetic glasses. Clays and Clay Minerals, 37, 348-354.

Upson, R., McAdam, J., and Clubbe, C. (2016) Climate Change Risk Assessment for Plants and Soils of the Falkland Islands and the Services they provide. Technical report. DOI: 10.13140/RG.2.2.15660.67203.

Wada, K. (1989) Allophane and imogolite. In: J.B. Dixon, and S.B. Weed, Eds., Minerals in Soil Environments, pp. 1051-1088. Soil Science Society of America, Madison, Wisconsin, USA.

Wang, C., Beke, G. J., and McKeague, J. A. (1978) Site characteristics, morphology and physical properties of selected ortstein soils from the Maritime Provinces. Canadian Journal of Soil Science, 58, 405–420.

Weaver, C.E. (1989) Clays, Muds, and Shales. Developments in Sedimentology 44. Elsevier, Amsterdam.

Wilson, M.J. (2004) Weathering of the primary rock-forming minerals: processes, products and rates. Clay Minerals, 39, 233-266.

Wilson, P. (1994) Origin, chronology and environmental significance of Holocene aeolian and alluvial sands at Blue Mountain, Falkland Islands. The Holocene, 4, 42–52.

Wilson, P. (2001) Rate and nature of podzolisation in aeolian sands in the Falkland Islands, South Atlantic. Geoderma, 101, 77–86.

Wilson, P., Bentley, M.J., Schnabel, C., Clark, R. and Xu, S. (2008) Stone run (block stream) formation in the Falkland Islands over several cold stages, deduced from cosmogenic isotope (^{10}Be and ^{26}Al) surface exposure dating. Journal of Quaternary Science, 23, 461–473.

Wilson. P., Clark, R., McAdam, J.H., and Cooper, E.A. (1993) Soil erosion in the Falkland Islands: an assessment. Applied Geography, 13, 329-352.

Worden, R.H., and Burley, S.D. (2003) Sandstone diagenesis: the evolution of sand to stone. In: S.D. Burley, and R.H. Worden, Eds., Sandstone Diagenesis: Recent and Ancient, pp. 3-44. Reprint Series Volume 4 of the International Association of Sedimentologists, Blackwell, London, UK.

Figures

Figure 1. Satellite photographs of the Falklands and of the exact location (square) of the investigated soil.

Figure 2. a) XRD patterns of the randomly oriented powder of one of the whole soil samples (top) and oriented mount of the corresponding < 2 μm size fraction (bottom). The background elevation in the latter may be due to the glass slide supporting the sample, the non-crystalline phase (see text) or both. b) Detail of the XRD patterns of the air-dry and glycolated mounts, showing the absence of expanding phyllosilicates. The figures in the labels are in Å. Alb: albite, Chl: chlorite, Felds: K-felspar, Kln: kaolinite, Mus: muscovite / illite, Phy: phyllosilicates, Qz: quartz.

Figure 3. a) Optical photograph of the thin section of the soil embedded in resin. b) SEM back-scattered electrons image of an area in the preparation shown in (a), including a grain and loose material around it. c-h) Maps of element abundance in the area in (b), where lighter contrast indicates higher element concentration.

Figure 4. SEM images and EDS spectra of the Falklands soil. The star symbols indicate the analyzed spots. a) Back-scattered electron image of a large clast with high Fe content (light contrast) surrounded by smaller clasts or aggregates and mineral matrix. b) Two mica grains with different Al-Mg content. c) Area within the large grain in a), showing two different types of occurrence of Fe oxides: an individual, well delimitated grain in spectrum 1 (Si, Al and K are probably from areas outside the grain) and a diffuse distribution of very small Fe oxide grains as illustrated with spectrum 2. d) Detail of the mineral fabric, with mineral grains and surrounding matrix of very fine grains. Spectrum 1,d identifies a muscovite grain. Spectrum 2,d is from the fine matrix.

Figure 5. Detailed SEM image, both from back-scattered electrons (a) and secondary electrons (b), of the texture within one of the clasts in the Falklands soil. There is a large quartz grain on the right and multiple mineral grains in the centre and left, with no preferential orientation. The top is the edge of the clast, where elongated particles are orientated approximately parallel to the surface. Light contrast areas in (a) correspond to Fe oxides.

Figure 6. SEM photographs (BSE) of the fraction < 2 μm of the Falklands soil and EDS spectra of selected points (indicated with an asterisk). The small particles in the background correspond to the non-crystalline silicate material (spectra 1,b; 1,c; and 1,d). The large particles are chlorite (b), moscovite (c) and kaolinite (d).

Figure 7. Atomic ratios from SEM-EDS analyses. The keys to all symbols are in (a). Map: average compositions obtained across each of the areas for which a chemical composition map was acquired in a thin section of the whole soil. The maps comprised areas of 1000 μm × 750 μm and 500 μm × 375 μm. Background: Chemical composition of areas (approximate squares with sides from a few μm to 30 μm) of the very fine material in the < 2 μm size fractions, including samples with (red symbols) and without (black symbols) removal of AO extractable Al and Fe. Oxides: mineral grains dominated by metal oxides. The other symbols correspond to mineral grains of recognizable mineralogy. Alb: albite, Chl: chlorite, Felds: K-felspar, Kln: kaolinite, Mus: muscovite / illite, Plag: plagioclase (higher Ca/Na than albite), Qz: quartz.

Table 1. Extractable Fe and Al in samples of the Falklands soil as measured by the dithionite-citrate-bicarbonate (DCB) and ammonium oxalate (AO) methods.

	DCB		AO			
	Fe	Al	Fe	Al	Fe_{AO} / Fe_{DCB}	Al_{AO} / Al_{DCB}
Sample	Atomic wt %					
II C Top	2.47 ± 0.20	1.04 ± 0.04	2.27 ± 0.04	2.04 ± 0.27	0.92	1.96
II H Top	2.13 ± 0.12	0.85 ± 0.08	1.75 ± 0.11	1.47 ± 0.16	0.82	1.73
II J Bot	2.78 ± 0.09	1.32 ± 0.03	2.22 ± 0.29	1.89 ± 0.09	0.80	1.43
II L Bot	2.06 ± 0.16	0.93 ± 0.13	1.79 ± 0.02	1.43 ± 0.24	0.87	1.54
Average	2.36 ± 0.07	1.04 ± 0.04	2.01 ± 0.08	1.71 ± 0.10	0.85	1.65

Top: Samples from the soil surface.
Bot: Samples from 5 cm below the soil surface.

Appendix text. Captions to the Appendix Figures.

Figure A.1. Representative, complete Podzol near the study site showing, from the top, a peaty O horizon, a thin leached E horizon, the spodic B horizon (Bs), and the B/S horizon grading into the underlying rock. In this profile there is a weakly developed iron pan layer below the E horizon.

Figure A.2. Surface of the sampled soil, probably corresponding to the B/C horizon of the profile in Figure A.1. The length of each side marked by the rope is 2 m.

Figure 1

Fig. 2

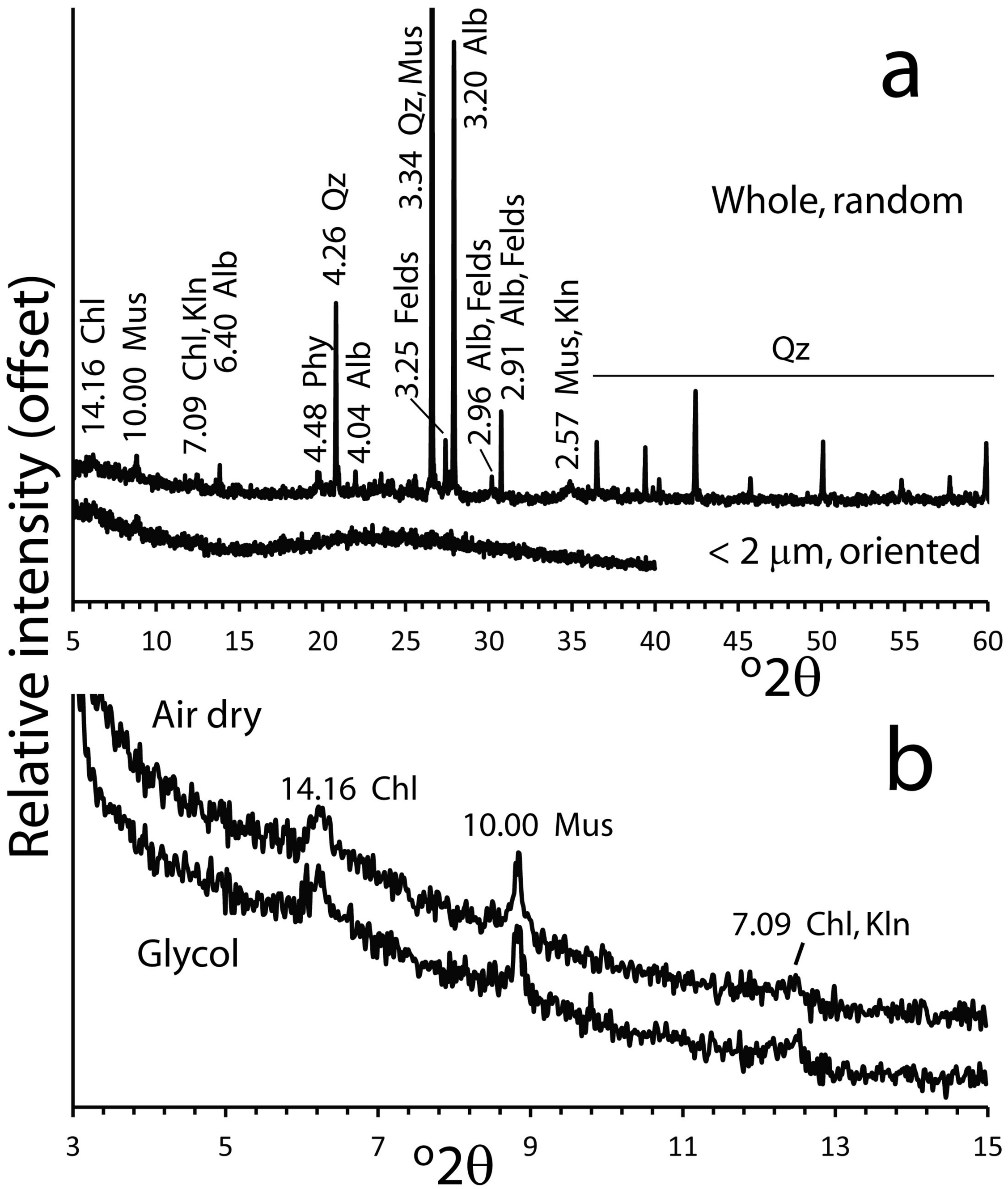
a
Whole, random
< 2 μm, oriented
Qz
14.16 Chl
10.00 Mus
7.09 Chl, Kln
6.40 Alb
4.48 Phy
4.26 Qz
4.04 Alb
3.25 Felds
3.34 Qz, Mus
3.20 Alb
2.96 Alb, Felds
2.91 Alb, Felds
2.57 Mus, Kln
Relative intensity (offset)
5 10 15 20 25 30 35 40 45 50 55 60
°2θ
b
Air dry
Glycol
14.16 Chl
10.00 Mus
7.09 Chl, Kln
3 5 7 9 11 13 15
°2θ

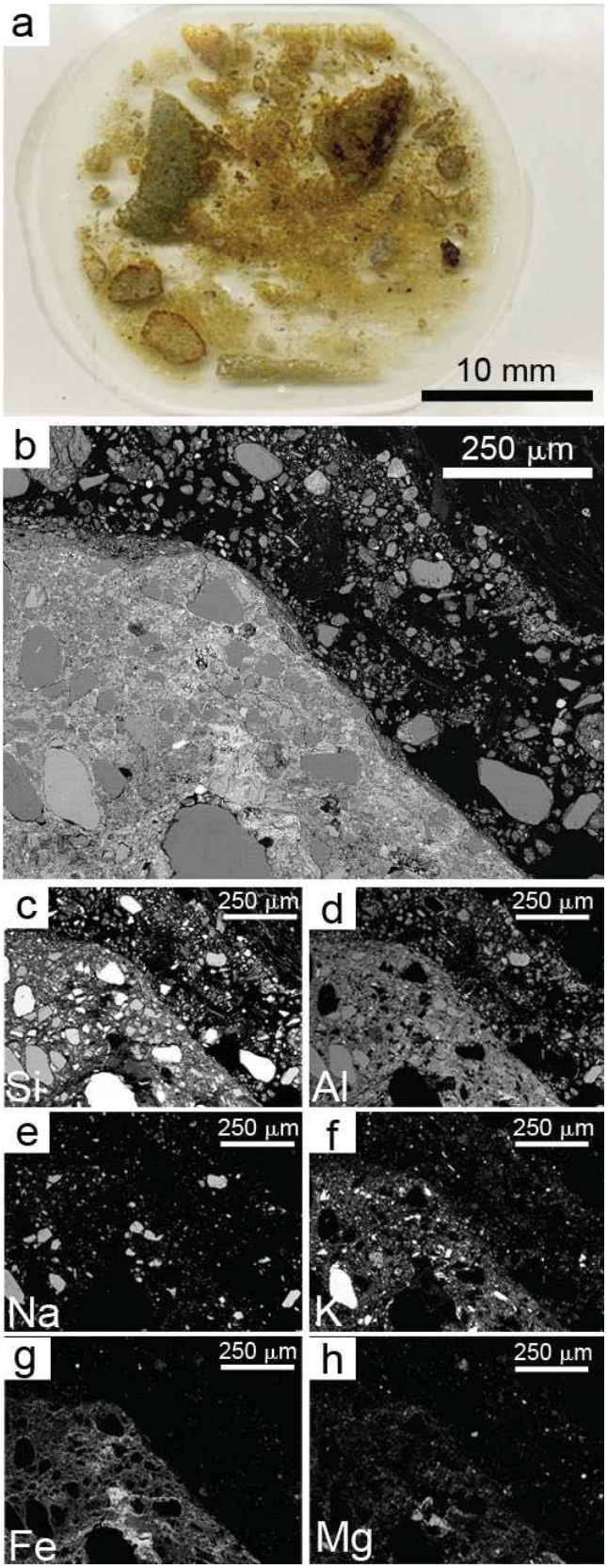
a
10 mm
b
250 μm
c
250 μm
Si
d
250 μm
Al
e
250 μm
Na
f
250 μm
K
g
250 μm
Fe
h
250 μm
Mg

Figure 3

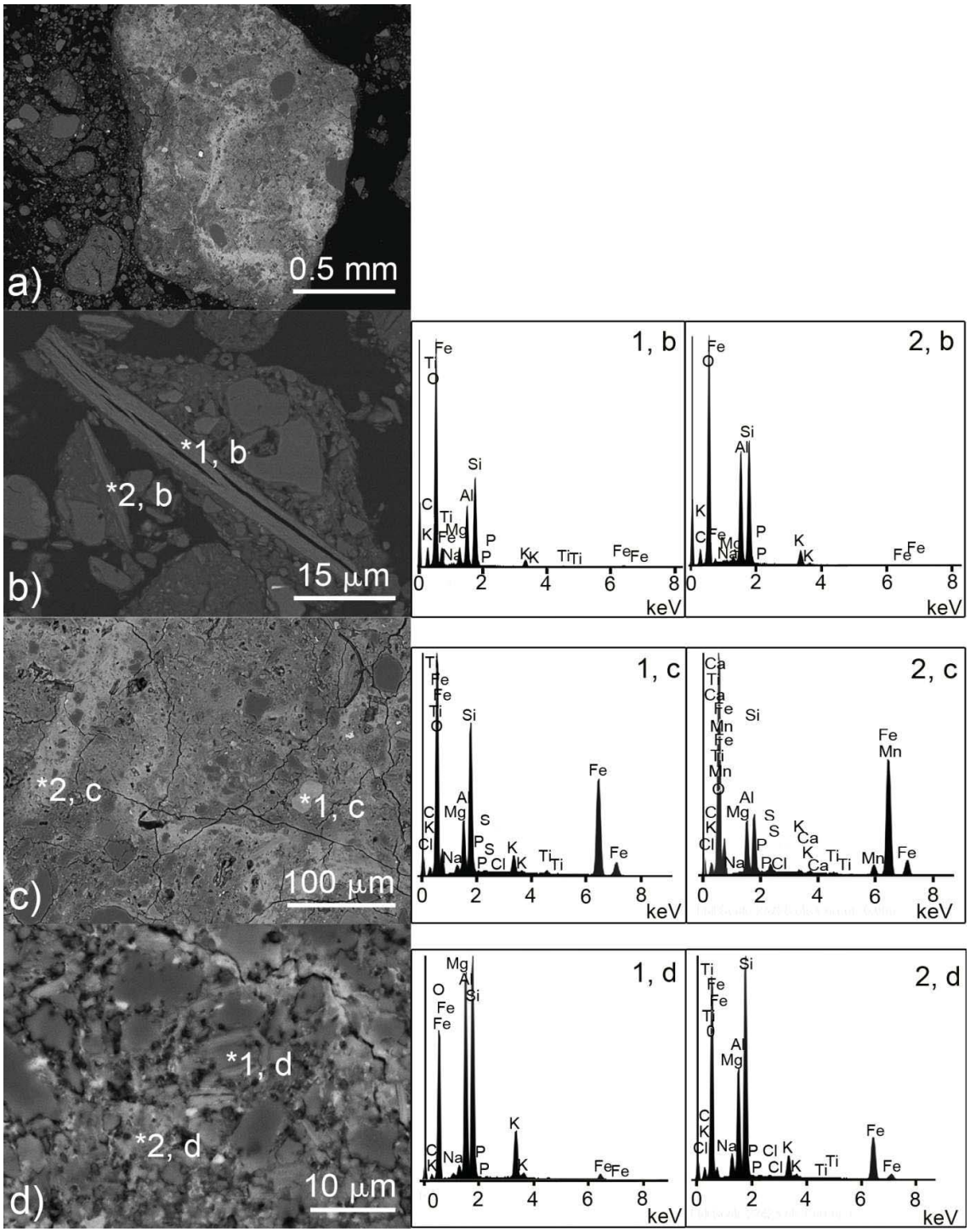

Figure 4

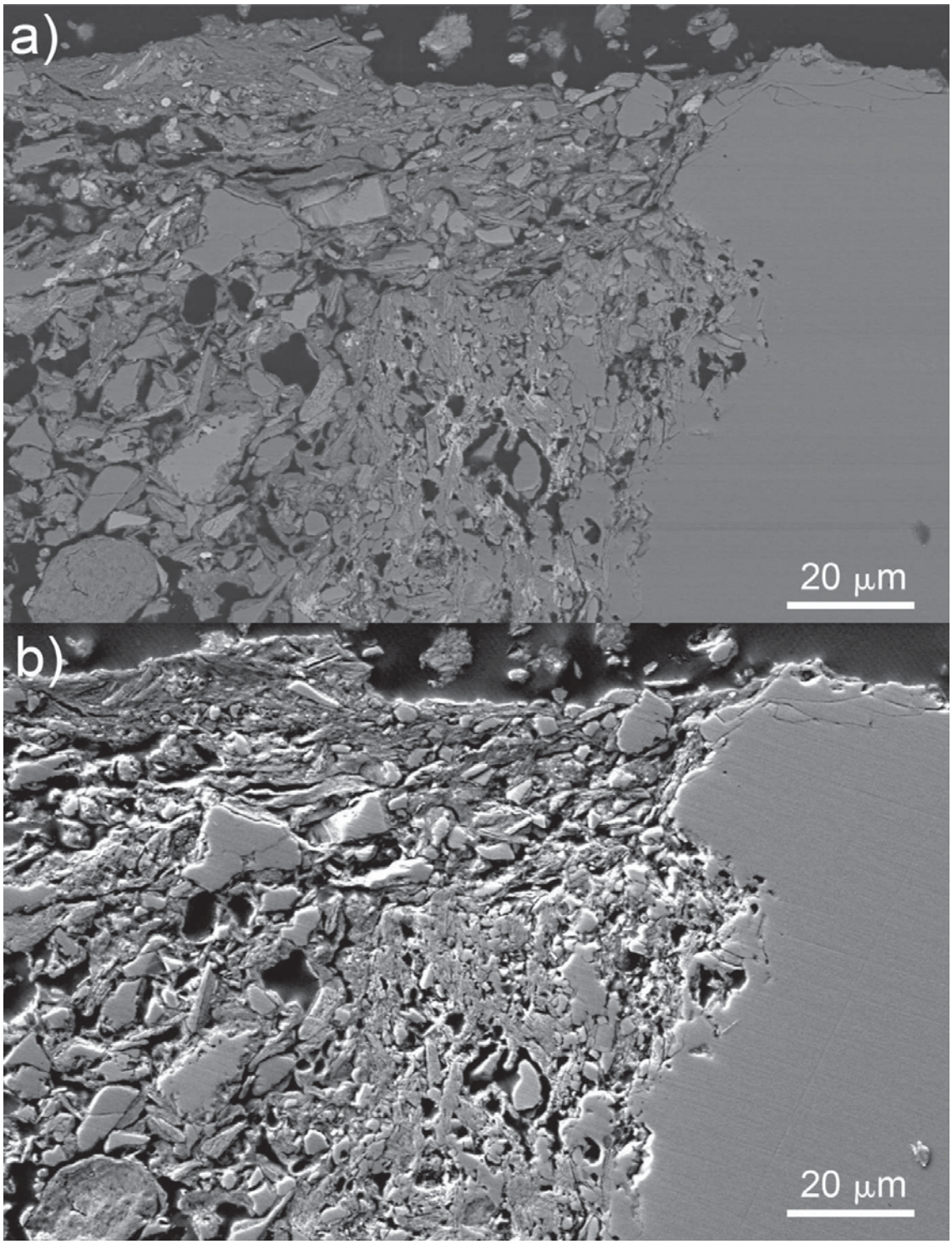

Figure 5

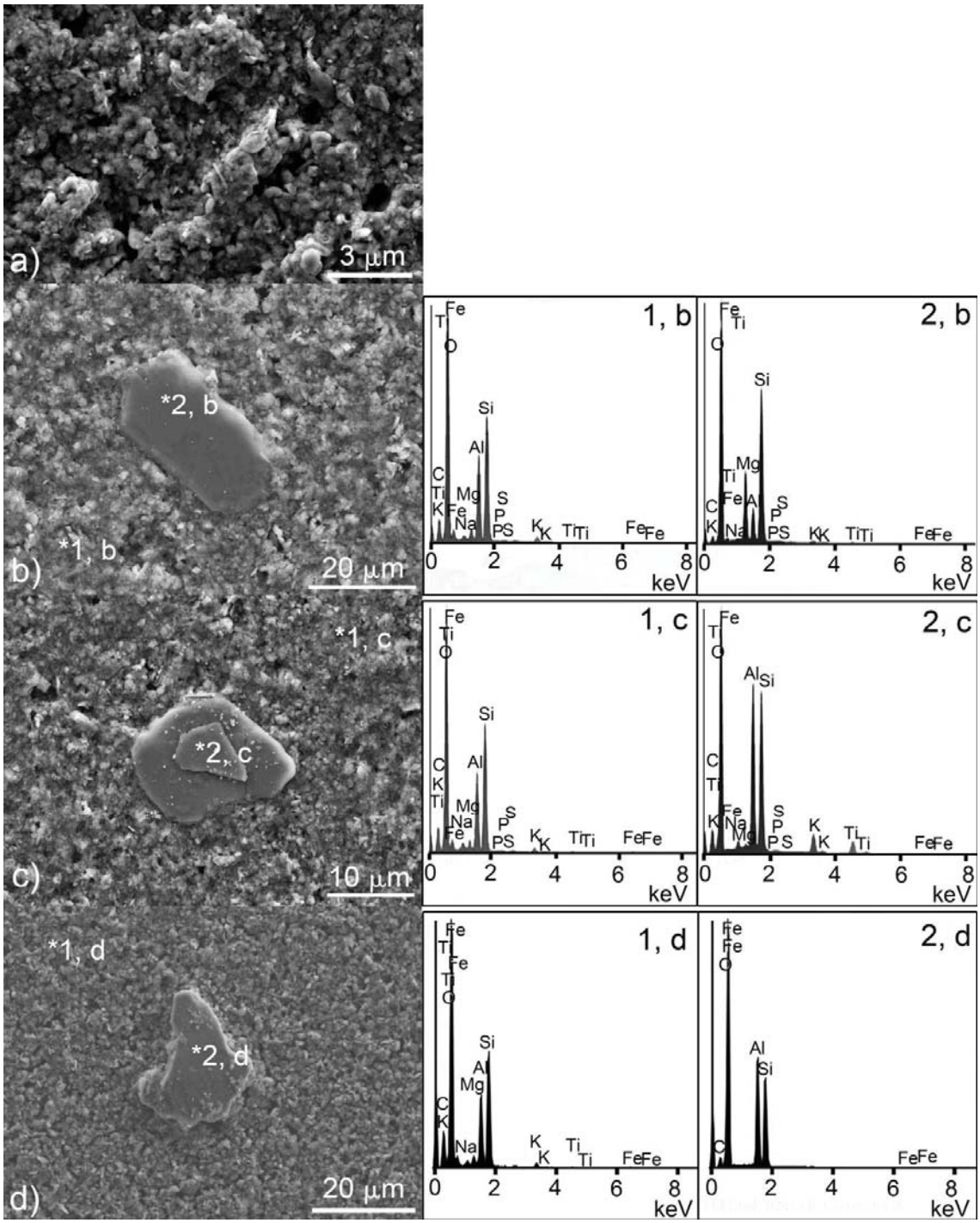

Figure 6

Fig. 7

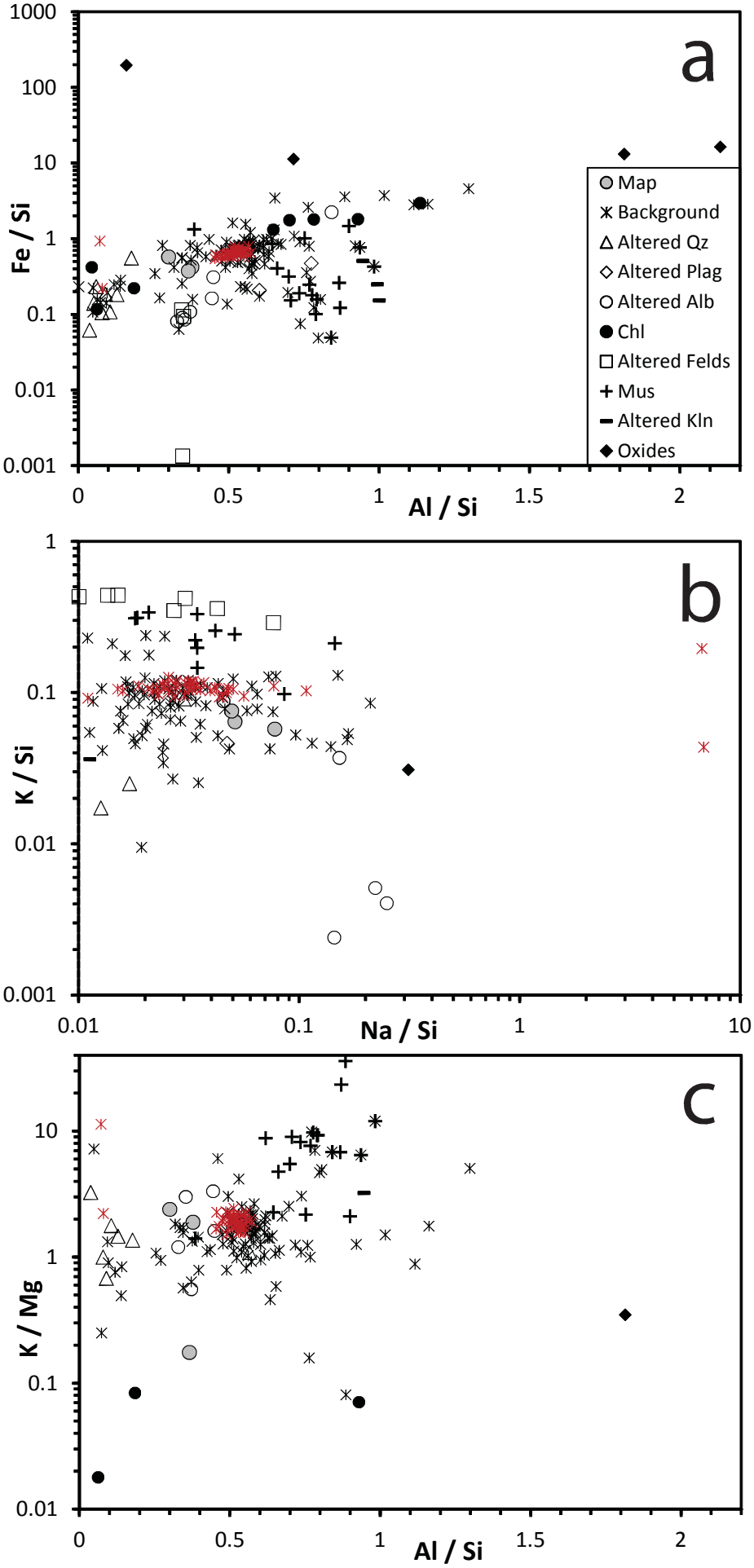
a
Fe / Si
Al / Si
Map
Background
Altered Qz
Altered Plag
Altered Alb
Chl
Altered Felds
Mus
Altered Kln
Oxides
b
K / Si
Na / Si
c
K / Mg
Al / Si